Ceramic Membrane Reactor for Synthesis Gas Production

J. T. Ritchie, J. T. Richardson, and Dan Luss
Dept. of Chemical Engineering, University of Houston, Houston, TX 77204

Membrane reactors enable synthesis-gas production from methane and air while avoiding the need for separation of the nitrogen either before or after the reaction. A stable membrane was developed by spray deposition of a dense thin film of $La_{0.5}Sr_{0.5}Fe_{0.8}Ga_{0.2}O_{3-\delta}$ on a high-purity porous α-alumina tube. The oxygen permeation rate at 850°C was 2.5×10^{-7} $mol\cdot cm^{-2}\cdot s^{-1}$. A quartz tube was placed coaxially around the membrane and the shell filled with a rhodium catalyst. Air was fed to the tube and methane to the shell. At 850°C the methane conversion was 97% and the selectivity to carbon monoxide approached 100%. Rapid radial mixing of the oxygen in the shell is essential to prevent coking and undesirable reactions. The membrane decomposes at 780°C in pure CH_4, but remains stable up to 970°C in a mixture of 90-mol % CH_4 and 10-mol % CO_2.

Introduction

Mixed ionic-electronic conducting (MIEC) perovskite oxides have several potential applications as catalytic membranes. Their oxygen permeability and catalytic activity make these membranes suitable for use in high-temperature partial oxidation reactions, such as methane oxidative coupling to higher hydrocarbons or partial oxidation of methane to synthesis gas (syngas). The main advantage of MIEC membrane reactors for these applications is that air can be used instead of oxygen, which avoids the expensive separation of the nitrogen either before or after the reaction. Also, the gradual introduction of oxygen reduces the contact with the partially oxidized products, which enhances the yield of the desired products.

Balachandran et al. (1995, 1997) conducted methane partial oxidation to syngas using the perovskite $SrFe_{0.2}Co_{0.8}O_{3-\delta}$ (SFCO) as a membrane. They obtained a methane conversion greater than 99% and CO selectivity of 98%. However, the SFCO membrane broke into several pieces at 850°C in the syngas environment. Pei et al. (1995) found that two types of fracture occurred. Shortly after the reaction started, a failure was caused by a lattice mismatch due to the oxygen gradient across the membrane. After a few days, a second type was induced by decomposition of the SFCO membrane to $SrCO_3$, Co, and Fe. This decomposition caused a large expansion, generating a crack along the tube axis. An ideal partial oxidation membrane should have high oxygen permeability, and chemical and lattice structure stability.

Mazanec (1997) reported that high oxygen fluxes could be obtained for some materials with the ABO_3 perovskite structure. A high level of acceptor doping of the A sites generates a large concentration of oxygen-ion vacancies, while doping the B sites by a small amount of Cr, Ti, or Mn enhances stability. Mazanec (1997) successfully used $La_{0.2}Sr_{0.8}Fe_{0.8}Cr_{0.2}O_{3-\delta}$ (LSFC) in syngas generation experiments for 500 h at 1,100°C. The disadvantage of this material is its low oxygen permeation rate (3.35×10^{-9} $mol\cdot cm^{-2}\cdot s^{-1}$ at 980°C under an oxygen partial-pressure gradient of 0.2 to 4×10^{-5} atm), which is smaller by a factor of 1,000 from than that of SFCO (Ming et al., 1998). Xu and Thomson (1998) and Tsai et al. (1997) have studied the oxygen permeability of a number of perovskite oxides, including $La_{0.6}Sr_{0.4}Fe_{0.8}Co_{0.2}O_{3-\delta}$ and $La_{0.2}Ba_{0.8}Fe_{0.8}Co_{0.2}O_{3-\delta}$, but none had both high permeability and stability. Material scientists are actively searching for new materials that have both high oxygen flux and high stability in the harsh environment encountered in syngas production.

The perovskite $La_{0.5}Sr_{0.5}Fe_{0.8}Ga_{0.2}O_{3-\delta}$ (LSFG) was reported by Ming et al. (1998) to have a higher oxygen permeation rate than LSFC but not as high as SFCO. However, the LSFG material is stable under low oxygen partial pressure, while SFCO quickly breaks down under these conditions.

Correspondence concerning this article should be addressed to D. Luss.

Bouwmeester and Burgraaf (1997) report that materials containing cobalt on the B site are normally not stable at low oxygen partial pressures. However, iron-doped materials are more stable than cobalt compounds. At 850°C, syngas has an oxygen partial pressure of $\sim 10^{-17}$ atm. Long-term stability of the membrane is necessary for this process to be industrially feasible.

In addition to having both high oxygen flux and good stability, it is essential to develop effective seals between the membrane and the connecting tubes. This is difficult due to the high temperature and ruggedness requirements. Qui et al. (1995) used gold and Mazanec (1997) used glass seals in laboratory experiments. However, these are not suitable for large-scale operation. The best solution is for the membrane and the connecting tubes to have the same expansion coefficients so they can be glued together with impermeable high-temperature cement.

Here we report a novel procedure for depositing a thin film (~ 150 μm) of LSFG onto a porous α-alumina substrate. This membrane tube is readily glued to nonporous α-alumina tubes using high-temperature cement. A reactor was constructed by placing a quartz tube coaxially around the membrane, and the shell was filled with a commercial 0.1% rhodium on alumina catalyst. The oxygen flux is among the highest values reported permeation rate through solid membranes, which remain stable under the very low oxygen partial pressure attained during syngas production.

Synthesis and Characterization of the Membrane Material

LSFG perovskite was produced by self-propagating high-temperature synthesis (SHS) from a mixture of solid powders [La_2O_3 (Aldrich, 99.9%), SrO_2 (Aldrich, ACS), Fe (Aldrich, 99.9+%), Ga_2O_3 (Johnson Matthey, 99.99%) and $NaClO_4$ (Johnston Matthey, ACS)] pressed to 50–60% of the theoretical density. The reaction

$$0.25La_2O_3 + 0.5SrO_2 + 0.1Ga_2O_3 + 0.8Fe + 0.2375\ NaClO_4 \rightarrow La_{0.5}Sr_{0.5}Fe_{0.8}Ga_{0.2}O_{3-\delta} + 0.2375NaCl_{(g)}, \quad (1)$$

was initiated by electrical heating of a chemical match of $Al_2O_3 + Ti + BaO_2$. The combustion was conducted in air with an internal oxygen supply from $NaClO_4$. White smoke was generated during the high-temperature combustion of the green reactant mixture due to the evaporation of NaCl. A detailed synthesis procedure is described by Ming et al. (1997, 1998, 1999). The production of LSFG by SHS is more economical than by conventional synthesis routes.

The phase composition and morphology of the samples were analyzed by X-ray diffraction (XRD), scanning electron microscope (SEM), and electron probe microanalysis (EPMA) (JEOL, JXA/8600). EPMA of the combusted sample showed that all the NaCl had evaporated during the high-temperature (1400°C) reaction (Figure 1). The sample was pure, uniform, and very close to the target stoichiometry of $La_{0.5}Sr_{0.5}Fe_{0.8}Ga_{0.2}O_{3-\delta}$.

In-situ high-temperature X-ray diffraction was conducted by a Siemens D5000 diffractometer equipped with a Buhler HDK 2.3 high-temperature stage and a Braun position-sensitive detector (PSD). The gas environment in the hot stage was controlled using four Tylan mass flow controllers and a Telfon mixing manifold. The material was tested for decomposition in a simulated syngas environment consisting of 22% CH_4, 57% H_2, and 21% CO_2 (for safety reasons, CO_2 replaced CO). Long-term stability must be maintained at 850°C in 10^{-17} atm oxygen, which is the equilibrium partial pressure of oxygen in syngas. Figure 2 shows that LSFG was stable in this highly reducing environment up to 900°C, at which it decomposes. The decomposition products generated above 900°C were $(LaSr)GaO_3$ and Fe. The parent structure, $LaFeO_3$, is stable up to 1,000°C in an oxygen partial pressure of 10^{-17} atm. Doping by Sr and Ga reduced its decomposition temperature to 900°C.

Similar experiments showed that LSFG decomposed at 780°C in pure methane and 660°C in pure hydrogen, but remained stable in air even at 1,300°C. This indicates that no

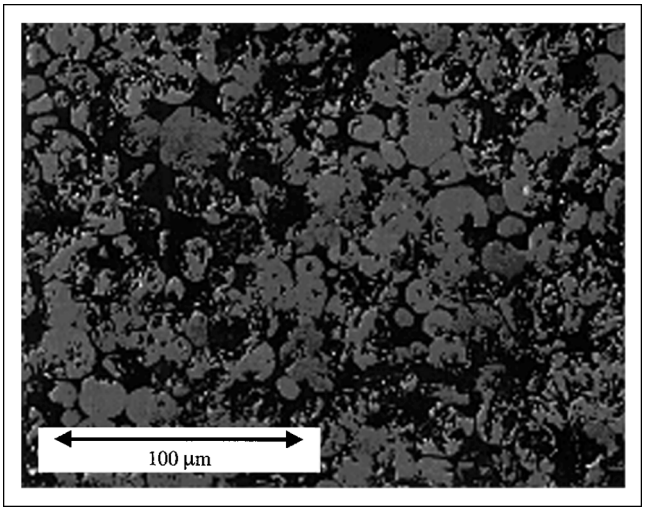

Figure 1. Backscattered electron image of $La_{0.491}Sr_{0.495}Fe_{0.824}Ga_{0.190}O_{3-\delta}$

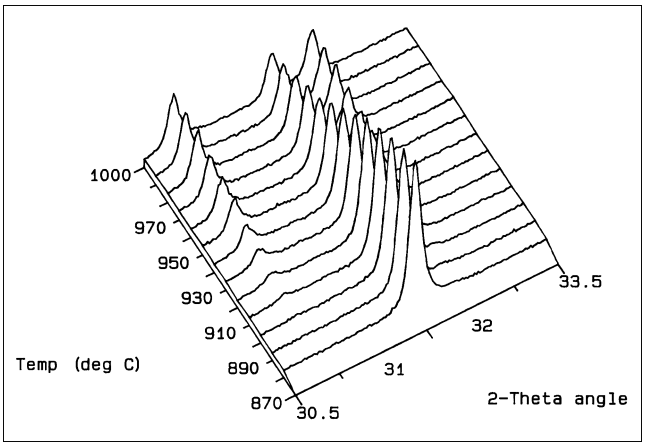

Figure 2. XRD patterns of powdered LSFG in 22% CH_4, 57%H_2, and 21% CO_2.

Sample was heated at 2°C/min and held at 10°C increments for 1 h from 870°C to 1,000 °C.

decomposition occurs when the catalyst is reduced in hydrogen at 600°C. However, decomposition will occur at 850°C using a pure methane feed unless a sufficient amount of oxygen permeates through the membrane and increases the oxygen partial pressure at the surface.

Synthesis of Thin-Film Membrane

We deposited a thin film of LSFG on a porous α-alumina tube and used this tube to construct the membrane reactor. To prepare the film, the SHS-produced powder was wet ground for 12 h in a Spex CertiPrep model 8000 Mixer/Mill using a tungsten carbide grinding vial. This reduced the average powder particle size to 5 microns. After grinding, the powder was mixed with isopropyl alcohol at 0.2 g/mL using a magnetic stir bar and a stir plate. The slurry was sprayed onto the exterior surface of a heated porous α-alumina tube (20 mm OD, 15 mm ID, 6.4 cm long) by a Paasche type VL airbrush. The tube was then sintered at 1,250°C for 4 h to get a uniform surface coverage. The membrane still had a few pinholes after three depositions (Figure 3a). To fill these pinholes, a vacuum was generated inside the tube and a dilute slurry (0.01 g/mL) of the powder was applied to the surface by a pipette. The tube was then sintered twice at 1300°C for 4 h to guarantee blockage of all the pinholes (Figure 3b). The reported film thickness is the average value around the tube, determined by a SEM of a cross-section of the tube. This deposition procedure generates a dense 150-μm-thick film.

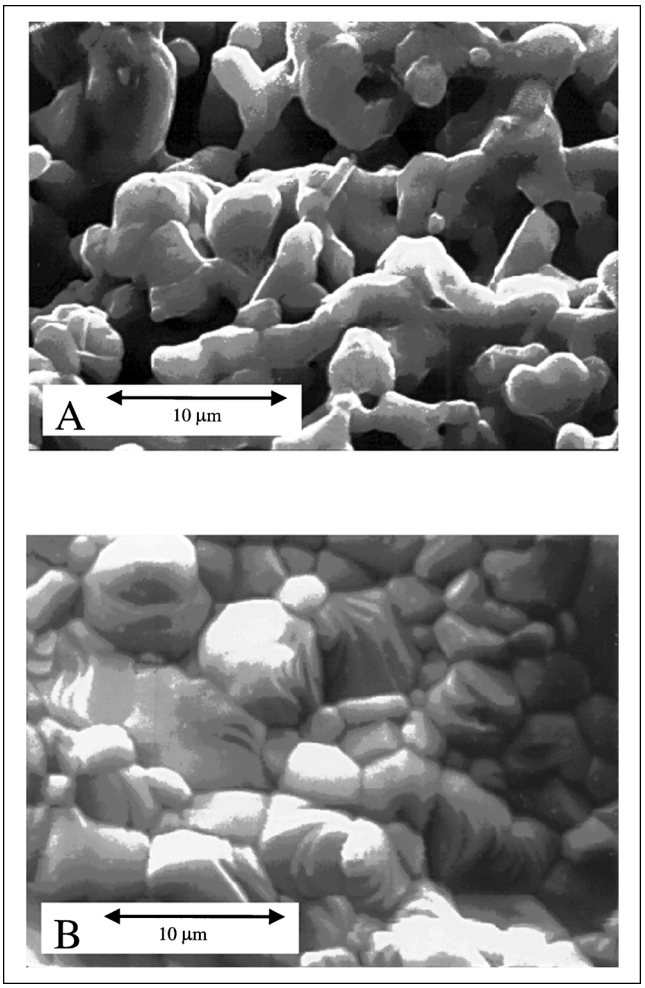

Figure 3. SEM image of the exterior surface of the tube after: (a) one deposition; (b)completion of deposition procedure.

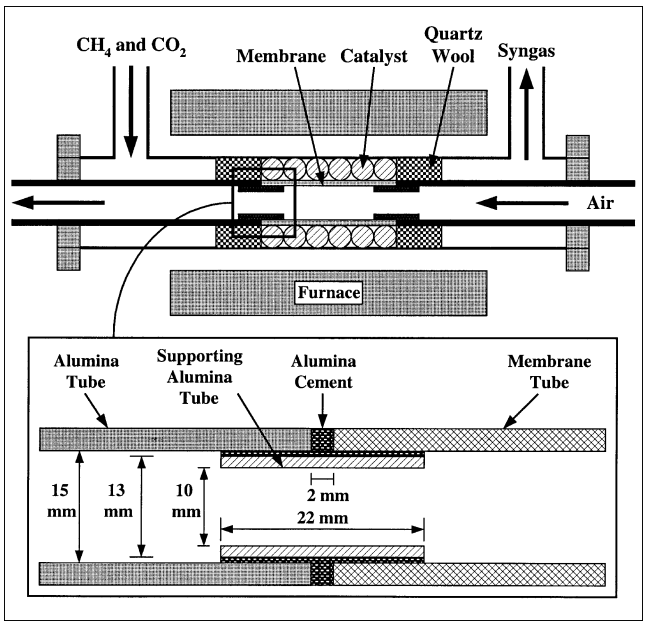

Figure 4. Membrane reactor used for methane partial oxidation.

Membrane material is deposited on the exterior of the porous alumina tube.

The membrane tube was glued to two nonporous high-purity α-alumina tubes by Haldenwanger high-temperature alumina cement. Two smaller tubes (13 mm OD, 10 mm ID, 2.5 cm length) were glued inside the tubes to support the seal (Figure 4). After curing, the tube was pressurized with hydrogen and checked for leakage. A reactor was constructed by placing a quartz tube around the membrane and placing a catalyst in the shell.

Membrane Reactor and Operation

Laboratory membrane reactors usually consist of either an isostatically pressed or extruded membrane connected to two tubes that are axially pressed against it, using a gold ring as a seal. These seals operate adequately in laboratories, but are not rugged enough for industrial applications. In our reactor, the 6.4-cm membrane is glued using high-temperature alumina cement to connecting tubes that have the same expansion coefficients (Figure 4). A small alumina tube is glued across the seal to provide axial strength. It extends for about 10 mm into both ends of the membrane. After the membrane is glued in place, a quartz tube was placed coaxially around the membrane and the tubes were held by Teflon fittings on the ends.

A catalyst was packed in the shell and held in place by quartz wool. We fed the methane mixture to the shell and air to the tube. The catalyst was 0.1% rhodium on 3.2-mm cylin-

drical alumina pellets purchased from Engelhard industries. Experiments were conducted with two different catalyst sizes: 10 μm and 3.2 mm. The 10-μm pellets were formed by grinding the 3.2-mm pellets in a mortar and pestle. This was done to enhance the contact of the catalyst with the walls of the membrane and minimize the diffusional resistance within the catalyst. When the 10-μm catalyst pellets were used, a relatively small quartz tube was placed around the membrane (24 mm ID and 28 mm OD) to minimize the distance (2 mm) between the membrane surface and the quartz tube, which minimized the radial oxygen gradient in the shell. This enhanced the conversion of the methane and decreased the coking of the catalyst. When the 3.2-mm catalyst pellets were used, a larger quartz tube had to be used (28 mm ID and 32 mm OD) to fit the larger pellets into the shell. The larger shell space (4 mm) increased the radial oxygen gradient. Adequate radial mixing is needed to get high methane conversion and to minimize coking.

The reactor was placed in a 970-W Lindberg tubular furnace and heated to 600°C. At this temperature, hydrogen was fed to the shell containing the catalyst at 85 cc/min (STP) for 3 h to reduce the rhodium to a pure metal state. After reduction, the reactor was flushed with nitrogen and the furnace heated to 850°C. After the furnace temperature was stable for 15 min methane was fed to the shell and air to the tube using Tylan mass-flow controllers. The effluent composition was monitored with an Anarad CO_2 IR, an Anarad CH_4 and CO IR, a Hewlett-Packard gas chromatograph, and an Ametek Quadrupole Mass Spectrometer.

Thermodynamic equilibrium calculations (Figure 5) showed that to obtain an effluent with only CO and H_2 from a stoichiometric feed of CH_4 and O_2 the reaction should be carried out around 1,000°C. Around 1,000°C the effluent composition approaches 2:1 H_2/CO and no CH_4 or CO_2. Due to LSFG decomposition, however, we are unable to run at this high temperature. At 850°C the H_2/CO ratio is still 2:1, but some CH_4, CO_2, $H_2O_{(g)}$, and $C_{(s)}$ remain. The 0.1% Rh on alumina catalyst reduces the CO_2 to undetectable levels. The Rh catalyst is very resistance to carbon coking but is not resistant to the water shift reaction. Thus, some water may form and decrease the H_2/CO ratio. The membrane decomposes at 850°C in pure methane. However, the permeation of oxygen through the membranes greatly increases the partial pressure of oxygen at the surface. When the oxygen flux is sufficiently high, the membrane remains stable under these conditions.

The oxygen flux depends on the bulk diffusion resistance of the membrane and the surface—exchange kinetics of the oxygen. Kim et al. (1999) found that the oxygen flux, Q (mol cm^{-2} s^{-1}) across the wall of a tubular membrane satisfies the relation

$$\frac{4\pi r_1 Q_1}{\langle cD_a \rangle} \ln\left(\frac{r_1}{r_2}\right) = \ln\left[\frac{\left(\frac{P_1}{p_0}\right)^n - \frac{2Q_1}{c_1 k_0}}{\left(\frac{p_2}{p_0}\right)^2 + \frac{2Q_2}{c_2 k_0}}\right], \qquad (2)$$

where p is the oxygen pressure at the interfaces, k is the equilibrium surface-exchange coefficient, the subscript 1 indicates the outer wall of the tube, the subscript 2 indicates the inner wall of the tube, and the subscript 0 indicates quantities evaluated at 1 atm oxygen pressure. The angular brackets, $\langle\ \rangle$, represent averaging over the chemical potential,

$$\langle cD_a \rangle = \frac{1}{\mu_1 - \mu_2} \int_{\mu_2}^{\mu_1} cD_a \, d\mu, \qquad (3)$$

where μ is the chemical potential of the oxygen ion–electron hole pairs at the two interfaces. Their experiments show that

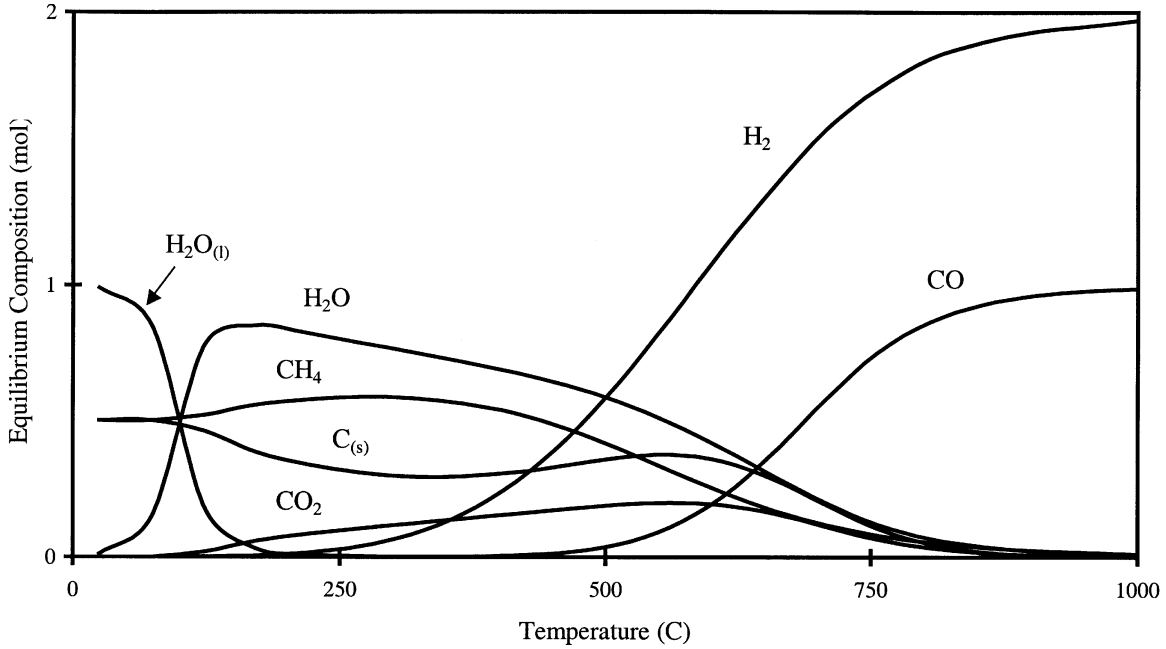

Figure 5. Calculated equilibrium behavior of a mixture of 2 mol CH_4 and 1 mol O_2 feed at 1 atm.

for oxygen transport through an LSFG membrane, n is 0.5. When the oxygen transport is limited by the rate of oxygen exchange between the gas and the membrane surface, Eq. 2 reduces to

$$Q_1 = \frac{r_2 k_0 c_1 c_2}{(r_1 + r_2)(c_1 + c_2)} \left[\left(\frac{p_1}{p_0} \right)^{1/2} - \left(\frac{p_2}{p_0} \right)^{1/2} \right]. \quad (4)$$

When the oxygen transport is limited by the bulk diffusion rate through the membrane, the oxygen flux is

$$Q_1 = \frac{\langle cD_a \rangle}{4r_1 \ln\left(\frac{r_1}{r_2} \right)} \ln\left(\frac{p_1}{p_2} \right). \quad (5)$$

Jacobson et al. (1998) found that an LSFG membrane of 2-mm wall thickness was surface = exchange limited. A detailed explanation of the surface–exchange kinetics and the governing flux equations is given by Kim et al. (1999). Assuming a constant oxygen flux along the membrane, complete consumption of the oxygen by the methane in the shell, via the reaction

$$CH_4 + \frac{1}{2} O_2 \rightarrow CO + 2H_2, \quad (7)$$

can occur only if the membrane velocity in the shell is at least

$$U_{CH_4} = \frac{2r_1 L Q_1 M_{CH_4}}{\rho_{CH_4}(R^2 - r_1^2)}, \quad (7)$$

where R is the inner diameter of the tube surrounding the membrane. The corresponding space velocity is

$$S = \frac{U_{CH_4}}{L}. \quad (8)$$

Experimental Results

Experiments were conducted to determine the oxygen permeation through a 2-mm-thick, 16-mm-ID, 6.4-cm-long isostatically pressed LSFG membrane tube and with a 150-μm thin membrane deposited on a porous α-alumina tube with 15 mm ID and 20 mm OD (Figure 6). The isostatically pressed tube and the film were made of the same powder. The powder was pressed and sintered at 1380°C for 10 h at a heating and cooling rate of 2°C/min, producing a tube with 97+% of the theoretical density. Gold seals were used at the connections between this tube and those connected to it. Air (0.21 atm O_2 at 20°C) was passed through the inside of the tube and helium, with a 10^{-5} atm O_2 impurity at 850°C, and was fed to the shell in which no catalyst was placed. This oxygen gradient across the membrane was smaller than when a methane mixture was fed to the shell. The highest oxygen permeation rate through the pressed tube was 1.2×10^{-7} mol $\cdot cm^{-2} \cdot s^{-1}$ at 900°C, while that through the thin membrane exceeded that to the thicker membrane by about two to four times, depending on the operating temperature. The highest oxygen flux through the thin membrane was 1.95×10^{-7} mol $\cdot cm^{-2} \cdot s^{-1}$ at 900°C. Higher fluxes are achieved with larger oxygen partial-pressure gradients. Methane has an oxygen partial pressure of $\sim 10^{-30}$ atm at 850°C, so it is expected that the oxygen flux through the membrane will increase when methane is fed to the shell. These experiments also checked that neither leakage through the seals nor cracks in the membrane occurred. We have not yet tested for repeatability of the experiments. These tests will be conducted in the near future.

The surface of the thin film looks as if formed by crystallization of molten material with many grain boundaries, while the surface of the pressed tube had fewer grain boundaries (Figure 7). In general, grain-boundary diffusion increases oxygen permeation. On the other hand, Sakai et al. (1996) found that the increase in the flux at the grain boundaries is small under the reducing environment existing during syngas

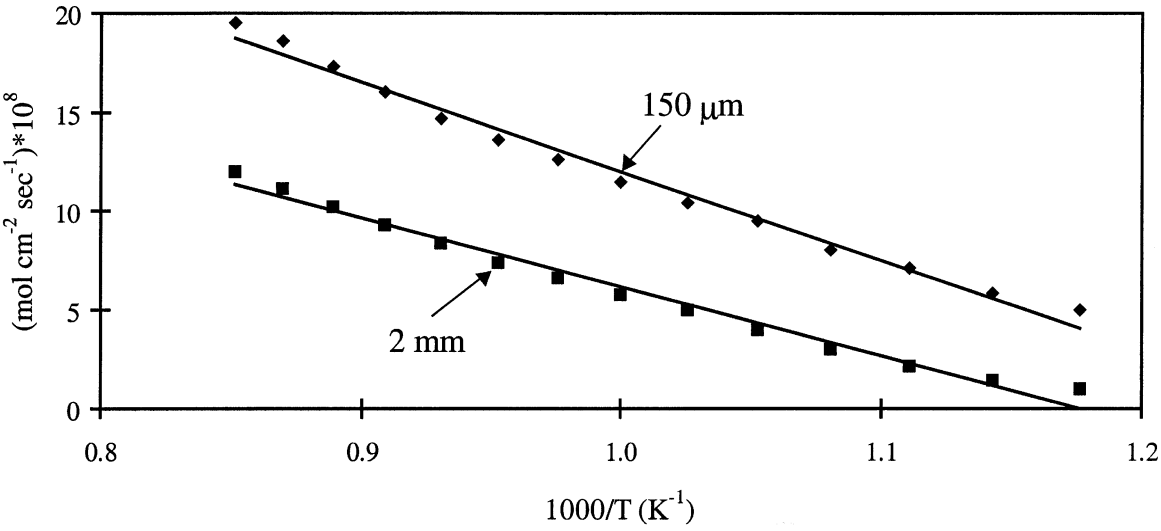

Figure 6. Oxygen permeation rates through a pressed tube and thin film with air (0.21 atm) inside the tube and helium (10^{-5} atm) in the shell.

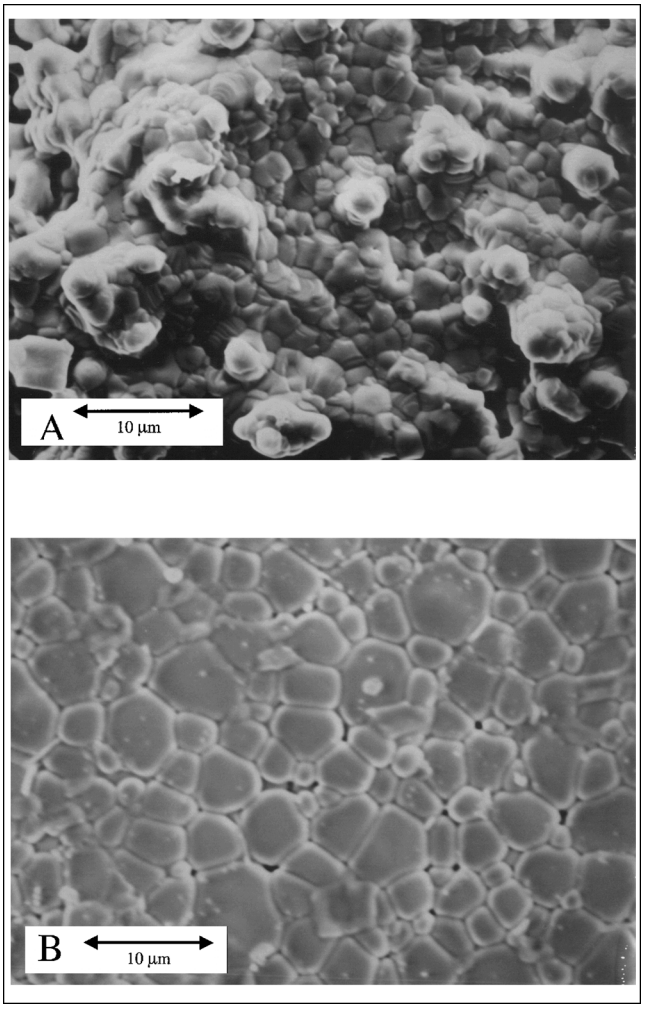

Figure 7. SEM image of the surface of: (a) thin film before any reaction; (b) pressed tube before any reaction.

production. A cross-sectional view of the pressed LSFG tube showed small voids, which increased the diffusional resistance. The deposition process of the film provided the LSFG powder adequate time to produce a dense, void, and pore-free film at the sintering temperature.

When the shell was filled with the 10-μm catalyst, syngas was produced by feeding methane to the shell and 150 cc/min (STP) air at a pressure of 3 psig to the tube. The same air flow rate was used in all experiments. The oxygen partial pressure decreases along the tube due to its consumption. Initially, pure methane was fed at the rate of 25 cc/min (STP). This is the stoichiometric amount needed to react when the oxygen permeation rate is 1.95×10^{-7} mol cm^{-2} s^{-1}, determined in the permeation experiments with helium. At these flow rates, the methane conversion was $>99\%$, the carbon monoxide selectivity, $CO/(CO+CO_2)$, 85%, and the H_2/CO ratio 1.5. The methane flow was then increased until the effluent stream consisted of only H_2, CO, and some unreacted CH_4. This occurred at 850°C for a CH_4 flow rate of 28 cc/min (STP). The corresponding space velocity was 0.17 s^{-1}. The highest oxygen permeation rate under the reaction conditions was 2.5×10^{-7} mol·cm^{-2}·s^{-1}. The methane conversion, selectivity to carbon monoxide, and the hydrogen to carbon monoxide ratio achieved by the reaction are shown in Figure 8 for various temperatures. Around 850°C, the methane conversion was 97% and the carbon monoxide selectivity approached 100%. The hydrogen to carbon monoxide ratio was only 1.8, due to production of some water. This water caused the catalyst particles to agglomerate and plug the reactor after 10 h online. The low hydrogen to carbon monoxide ratio may be due to the uncontrolled axial variation in the rate of oxygen fed into the shell. This variation may form regions within the reactor in which the oxygen concentration is either deficient or rich promoting the undesired oxidation of hydrogen. To prevent plugging of the reactor and enable extended operation, the 3.2-mm catalyst pellets were used in all subsequent experiments.

When exposed to pure methane, the membrane cracked at 780°C. When oxygen permeated through the membrane, however the oxygen partial pressure at the surface of the membrane exceeded that in the bulk of the methane feed and prevented the membrane decomposition. When the membrane was glued to the connecting nonporous tubes, a small alumina tube was glued across the seals to support the connections, as shown in Figure 4. These supporting tubes extend for about 10 mm into both ends of the 6.4-cm membrane. In that area, the lower oxygen flux caused LSFG decomposition and cracks to form in the upstream section of the membrane (Figure 9).

Figure 10 shows the thermodynamic equilibrium composition of a mixture of 0.9 mol CH_4, 0.1 mol CO_2, and 0.45 mol O_2. The equilibrium oxygen partial pressure in this mixture is 10^{-17} atm at 850°C instead of the 10^{-30} atm in pure methane at 850°C. The highest H_2/CO ratio attainable with this feed is 1.8 when no water production and side reactions occur. To circumvent membrane cracking, we fed the shell with a mixture of 90-mol % CH_4 and 10-mol % CO_2. *In situ* high-temperature XRD showed that the membrane was stable up to 970°C under this higher oxygen partial pressure and did not decompose at 850°C.

A series of experiments was conducted using the large (3.2-mm) catalyst pellets in which 25 cc/min (STP) methane was fed to the shell and 150 cc/min (STP) air to the tube (Figure 11). The highest permeation rate through the film under these conditions was 2.0×10^{-7} mol cm^{-2} s^{-1}. The corresponding methane mixture velocity through the shell, computed by Eq. 7, was 0.14 cm/s, or a space velocity of 0.02 s^{-1}. The slow velocity of the methane mixture through the shell did not generate efficient oxygen radial mixing. The inefficient radial mixing caused coke formation and allowed contact between the H_2 and unreacted O_2, which caused water formation and reduced the H_2/CO ratio to 1.63 instead of the theoretical limit of 1.8. The corresponding methane conversion was 91%. This poor reactor performance may be enhanced by improving the radial mixing by increasing the velocity through the shell of the laboratory reactor. The flow rate of methane cannot be increased above the stoichiometric amount with the permeated oxygen without decreasing its conversion. However, if a one-meter-long membrane tube is used, a methane flow rate of about 400 cm^3/min (STP) is needed to convert the oxygen. This corresponds to a line velocity of 2.2 cm/s or a space velocity of 0.02 s^{-1}. Clearly, the velocity in the meter-long reactor would be much higher (2.2 cm/s) than that

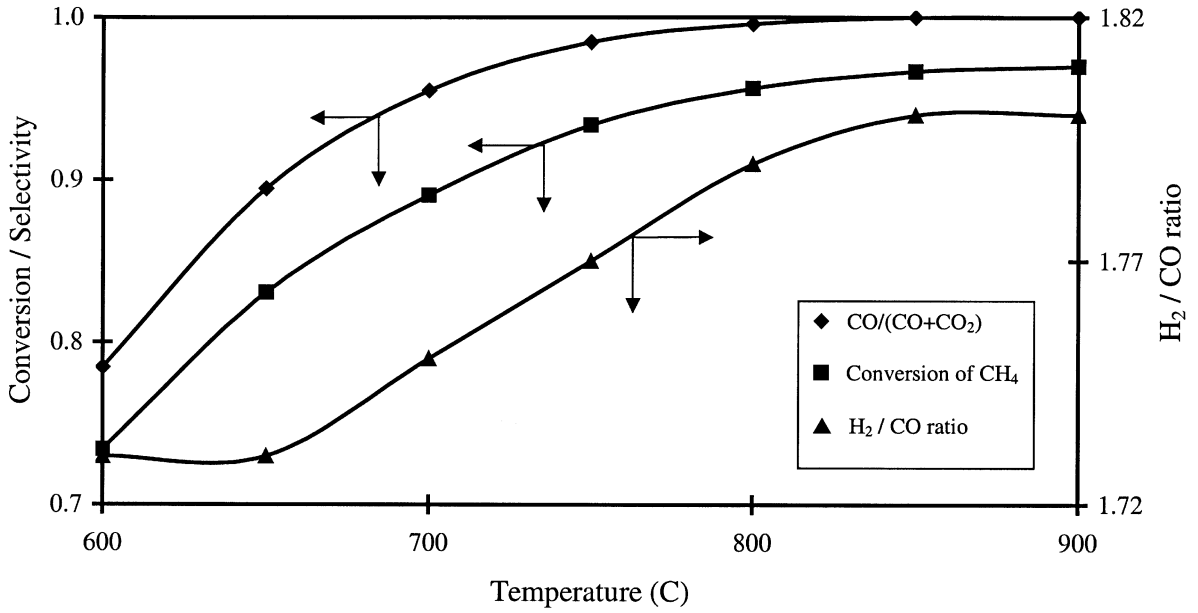

Figure 8. Impact of reactor temperature on conversion of pure CH_4 feed, selectivity of CO ($CO/(CO+CO_2)$), and H_2/CO ratio during syngas production using 10-μm Rh catalyst.

in our laboratory reactor (0.14 cm/s) at the same space velocity. This higher velocity would improve the mixing and increase the conversion. To test this, a nonreactive diluent, helium, was added to the methane feed. This raised the gas velocity in the shell to 0.41 cm/s (space velocity of 0.06 s^{-1}). The higher velocity increased the mixing of the reactants in the shell and significantly enhanced the performance of the reactor (Figure 12). The methane conversion reached 98% and the CO_2 was undetectable. The H_2/CO ratio increased to 1.76, which is rather close to the theroetical limit of 1.8. This enhanced performance proves that the poor radial mixing of the oxygen in the catalyst bed is due to the very slow velocity of the reactants through the shell. In our experiments, we used helium to increase the velocity through the shell. This use of an inert will not be necessary in an industrial reactor, as at the same space velocity, a much higher methane velocity will be used in a longer reactor.

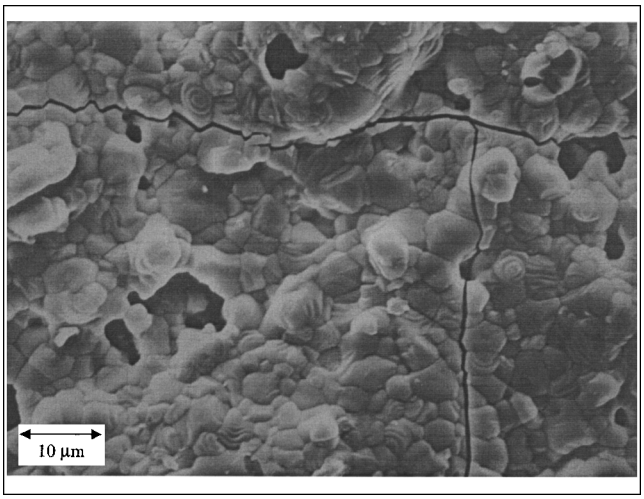

Figure 9. Surface of the upstream section of membrane after use in syngas production at 850°C with pure methane feed and 10-μm Rh catalyst.

The 3.2-mm rhodium catalyst pellet is almost as large as the annular space (4 mm). Thus, we used a smaller catalyst to determine the influence of catalyst size on the conversion. We packed the reactor shell with 2-mm spherical alumina pellets impregnated with 0.1% rhodium and fed it with a 90-mol % CH_4 and 10-mol % CO_2 mixture. With no diluent added to increase the velocity through the reactor, the selectivity to CO was about 99%, the CH_4 conversion was about 95%, and the H_2/CO ratio was about 1.67. The rhodium catalyst has a high resistance to coking, but it is not resistant to further oxidation of the partially oxidized products. While the enhanced mixing may improve the CO selectivity and CH_4 conversion, it appears that only an increase of the velocity through the reactor or use of a different catalyst can significantly improve the H_2/CO ratio.

Our membrane reactor is much more rugged than those reported in the literature. The membrane film and seals did not fail following rapid cooling at a rate of up to 10°C/min and following heating at a rate of 5°C/min. The reactor did not fail following tapping, which was used to simulate mild vibration in an industrial environment. The membrane and the substrate are two different materials. While short-term ($\sim$ 29 days) reaction between them did not lead to any degradation in the membrane performance, long-term (10 years) stability has not yet been tested. Another problem is the sealing cement, which is water-soluble. The oxidation of the products produces water, which slowly dissolves the seal. In our experiments the seal began to leak after 700 h of operation, or about 29 days. Industrial operation of the membrane

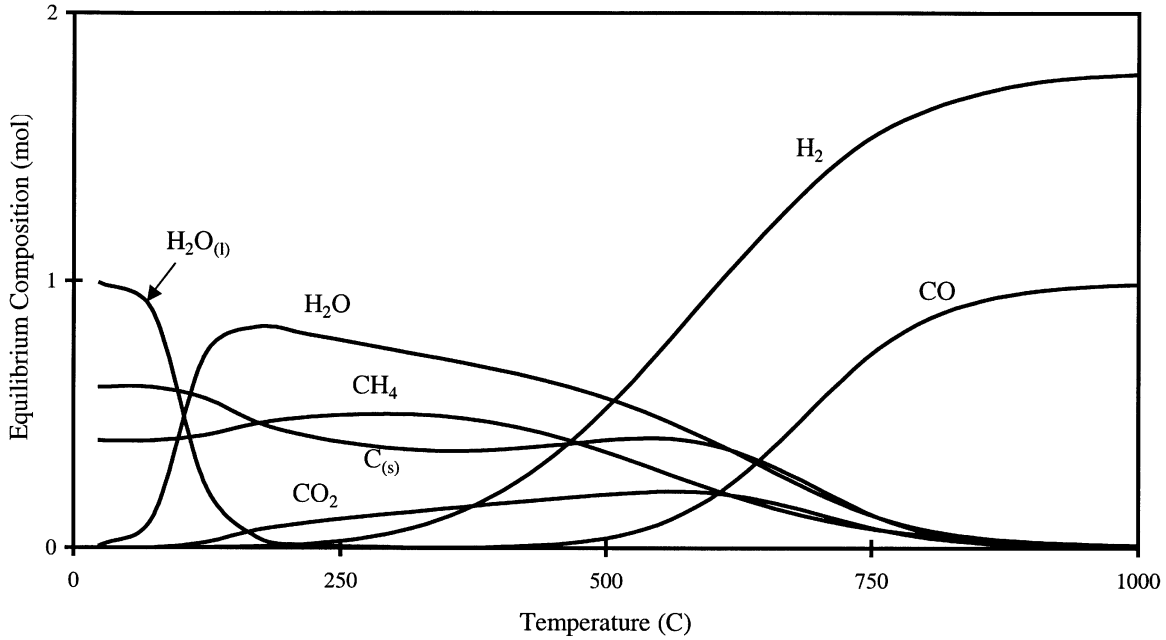

Figure 10. Calculated equilibrium composition of a mixture of 0.9 mol CH_4, 0.1 mol CO_2, and 0.45 mol O_2 feed.

reactor will require long-term stability and discovery of water-resistant sealant.

Conclusions

A membrane reactor offers several potential advantages for the production of syngas. The main advantage is avoiding the need to separate the nitrogen either from the air or from the effluent stream. Development of such a reactor requires finding a membrane selective for oxygen, which has a high permeation rate and that remains stable under the low oxygen partial pressure. Moreover, the material should enable production of a very thin membrane with no pinholes, which can be readily connected to the tubes supplying the feed and removing the effluents.

Our experiments show that such a membrane can be produced from $La_{0.5}Sr_{0.5}Fe_{0.8}Ga_{0.2}O_{3-\delta}$ by spray deposition on an inert alumina tube. The flux of the oxygen determines the corresponding feed rate of the methane. Assuming that only the syngas reaction occurs, the methane was fed at a stoichiometric rate of 1 mol methane to 0.5 mol oxygen. Using a 0.1% Rh on alumina catalyst, we were able to obtain high conversions of the methane (98%), high H_2/CO ratio (1.76), and high CO selectivity ($\sim$100%). The experiments showed

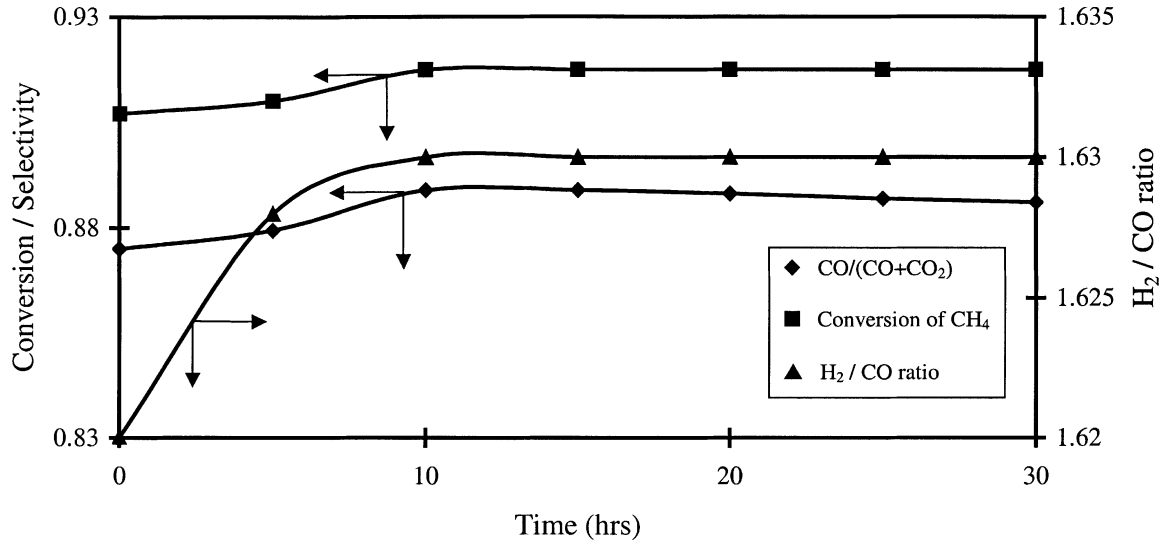

Figure 11. Conversion of pure CH_4 feed, selectivity of CO ($CO/(CO+CO_2)$), and H_2/CO ratio during syngas production at 850°C using 3.2-mm Rh catalyst.

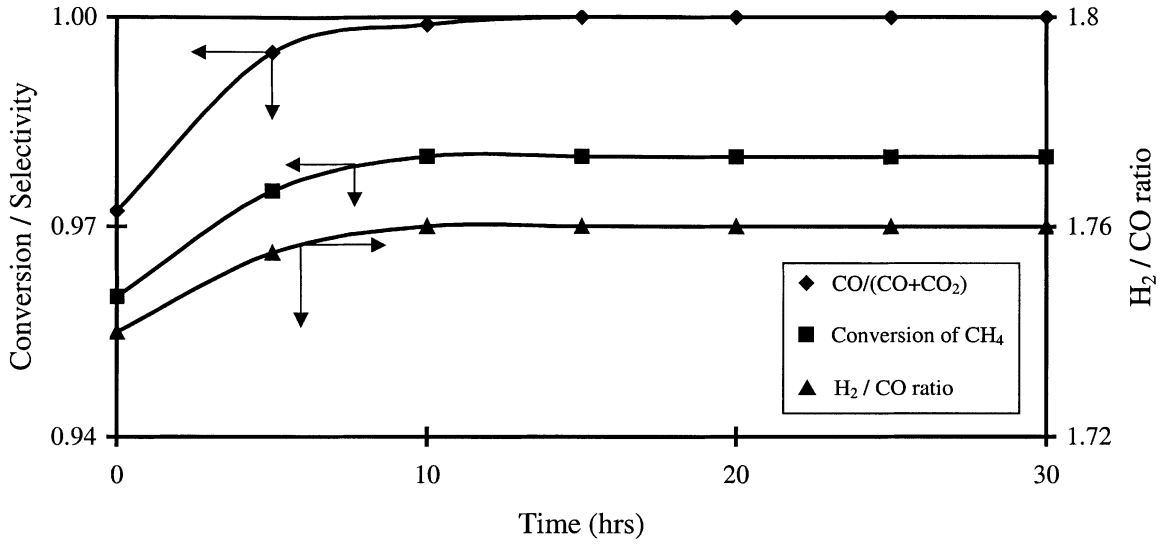

Figure 12. Conversion of pure CH_4 feed, selectivity of CO [$CO/(CO+CO_2)$], and H_2/CO ratio during syngas production at 850°C using 3.2-mm Rh catalyst and feeding helium at 50 cm^3/min (STP).

that in order to obtain a high performance and avoid coke formation, it is essential to minimize the radial gradients of the oxygen in the catalyst bed. We accomplished this in our short laboratory membrane reactor either by using a fine catalyst powder (10 μm) in a relatively narrow (2 mm) annular catalyst bed, or by adding helium to increase the velocity and radial mixing, when larger catalyst pellets in a wider shell (4 mm) were used. The addition of an inert to improve the mixing will not be needed in industrial reactors because these longer reactors will operate at higher velocities than in our short laboratory reactor.

The experiments showed that cracking of the LSFG membrane may occur just at the inlet to the reactor if the support of the connectors of the membrane to the feed tube decreases the oxygen permeation at that point. This cracking may be circumvented by addition of carbon dioxide or oxygen to the feed.

Our preliminary experiments suggest that it should be possible to develop a commercial process for production of syngas by a membrane reactor. Additional experiments will be needed to optimize its performance. The membrane production procedure developed by us can be readily applied to manufacture membranes from other ceramic materials that may have superior properties.

Acknowledgments

This work was supported in part by the MRSEC program of the National Science Foundation under Award Number DMR-9632667 and the State of Texas through the Texas Center for Superconductivity at the University of Houston.

Notation

c = concentration of oxygen ions, $mol \cdot cm^{-3}$
D_a = diffusion coefficient of the oxygen ion–electron hole pairs, $cm^2 \cdot s^{-1}$
k = equilibrium surface exchange coefficient, $cm \cdot s^{-1}$
L = membrane tube length, cm
M_{CH_4} = molecular weight of methane, $g \cdot mol^{-1}$
n = order of the chemical reaction at the gas–membrane interface
p = oxygen partial pressure, atm
Q = oxygen flux, $mol \cdot cm^{-2} \cdot s^{-1}$
R = outer radius of the shell, cm
r = radius of the tubular membrane, cm
S = space velocity of the methane, s^{-1}
U_{CH_4} = velocity of methane in the shell, $cm \cdot s^{-1}$

Greek letters

ρ_{CH_4} = density of methane, $g \cdot cm^{-3}$
μ = chemical potential of the oxygen ion–electron hole pairs

Subscripts

0 = quantity evaluated at 1 atm oxygen pressure
1 = outer wall of membrane tube
2 = inner wall of membrane tube

Literature Cited

Balachandran, U., J. T. Dusek, S. M. Sweeney, R. B. Poeppel, R. L. Mieville, P. S. Maiya, M. S. Kleefisch, S. Pei, T. P. Kobylinski, C. A. Udovich, and A. C. Bose, "Methane to Syngas via Cermaic Membranes," *Amer. Ceram. Soc. Bull.*, **74**, 71 (1995).

Balachandran, U., J. T. Dusek, P. S. Maiya, B. Ma, R. L. Mieville, M. S. Kleefisch, and C. A. Udovich, "Ceramic Membrane Reactor for Converting Methane to Syngas," *Catal. Today*, **36**, 265 (1997).

Bouwmeester, H. J. M., and A. J. Burgraaf, *The CRC Handbook of Solid State Electrochemistry*, CRC Press, and Boca Raton, FL (1997).

Jacobson, A. J., S. Kim, A. Medina, Y. L. Yang, and B. Abeles, "Dense Oxide Membranes for Oxygen Separation and Methane Conversion," *Mater. Res. Soc. Symp. Proc.*, **497**, 29 (1998).

Kim, S., Y. L. Yang, A. J. Jacobson, and B. Abeles, "Oxygen Surface Exchange in Mixed Ionic Electronic Conductor Membranes," *Solid State Ionics*, **121**, 31 (1999).

Mazanec, T. J., "Electropox Gas Reforming," *Proc. Int. Conf. on Ceramic Membranes*, H. U. Anderson, A. C. Khandkar, and M. Liu, eds., Electrochemical Society, Pennington, NJ, p. 16 (1997).

Ming, Q., M. D. Nersesyan, K. Ross, J. T. Richardson, and D. Luss, "Reaction Steps and Microstructure Formation During SHS of $La_{0.8}Sr_{0.2}CrO_3$," *Combust. Sci. Technol.*, **128**, 279 (1997).

Ming, Q., J. Hung, Y. L. Yang, M. D. Nersesyan, A. J. Jacobson, J. T. Richardson, and D. Luss, "Combustion Synthesis of $La_{0.2}Sr_{0.8}Cr_{0.2}Fe_{0.8}O_{3-x}$," *Combust. Sci. Technol.*, **138**, 279 (1998).
Ming, Q., M. D. Nersesyan, A. Wagner, J. Ritchie, J. T. Richardson, and D. Luss, "Combustion Synthesis and Characterization of Sr and Ga Doped $LaFeO_3$," *Solid State Ionics*, **122**, 113 (1999).
Pei, S., M. S. Kleefisch, T. P. Kobylinski. J. Faber, C. A. Udovich, V. Zhang-McCoy, B. D. Dabrowski, U. Balachandran, R. L. Mieville, and R. B. Poeppel, "Failure Mechanisms of Ceramic Membrane Reactors in Partial Oxidation of Methane to Synthesis Gas," *Catal. Lett.*, **30**, 201 (1995).
Qui, L., T. H. Lee, L. M. Liu, Y. L. Yang, and A. J. Jacobson, "Oxygen Permeation Studies of $SrCo_{0.8}Fe_{0.2}O_{3-x}$," *Solid State Ionics*, **76**, 321 (1995).
Sakai, N., T. Horita, H. Yokokawa, M. Dokiya, and T. Kawada, "Oxygen Permeation Measurement of $La_{1-x}Ca_x\ CrO_{3-\delta}$ by Using an Electrochemical Method," *Solid State Ionics*, **86**–**88**, 1273 (1996).
Tsai, C. Y., A. G. Dixon, W. R. Moser, and Y. H. Ma, "Dense Perovskite Membrane Reactors for Partial Oxidation of Methane to Syngas," *AIChE J.*, **43**, 2741 (1997).
Xu, S. J., and W. J. Thomson, "Stability of $La_{0.6}Sr_{0.4}Co_{0.2}Fe_{0.8}O_{3-d}$ Perovskite Membranes in Reducing and Nonreducing Environments," *Ind. Eng. Chem. Res.*, **37**, 1290 (1998).

Manuscript received Nov. 13, 2000, and revision received Apr. 9, 2001.